MSE-Optimal Power Allocation in Wireless Sensor Networks for Field Reconstruction Based on Shift-Invariant Spaces

Günter Reise*, Javier Matamoros†, Carles Antón-Haro†, and Gerald Matz*
*Institute of Telecommunications, Vienna University of Technology, Vienna, Austria, {guenter.reise;gerald.matz}@tuwien.ac.at
†Centre Tecnològic de Telecomunicacions de Catalunya (CTTC), Castelldefels, Spain, {jmatamoros;canton}@cttc.es

***Abstract*—In our previous work, we developed field reconstruction methods in wireless sensor networks based on shift-invariant spaces. In this paper, we use amplify-and-forward for the transmission of the sensor node measurements to the fusion center and we derive the mean square error (MSE) of the reconstructed field as a function of the measurement noise, the channel gains between sensor nodes and fusion center, the receiver noise variance, and the sensor placement. Imposing a sum-power constraint, we formulate the MSE-optimal power allocation as a convex optimization problem that can be solved numerically. For the case of critical sampling we derive a closed-form expression for the optimal power allocation. For Gaussian channels and Rayleigh-fading channels, we compare the performance of the proposed power allocation schemes and uniform power allocation. The power allocation schemes provide new insights for our field reconstruction scheme and feature excellent performance while being easy to implement.**

I. Introduction

Wireless sensor networks (WSN) have attracted considerable attention in recent years as solution to distributed inference for diverse monitoring applications [1]. Sensor nodes are deployed in the region to be monitored and communicate wirelessly in order to collect and process information about the physical quantity of interest. In this paper, we deal with the reconstruction of physical fields from spatial samples provided by the sensor nodes in a WSN. We use the system architecture introduced in [2] for distributed sampling and reconstruction of a two-dimensional (2-D) physical field based on shift-invariant spaces.

The goal of power allocation is to optimally assign transmit powers to the sensor nodes of the WSN, either in order to minimize the estimation error subject to a sum-power constraint or in order to minimize the transmit power subject to a distortion target. Such problems have been extensively investigated in the literature for linear scalar models. In particular, the power scheduling for uncoded quadrature amplitude modulated (QAM) transmission was studied in [3]. Power allocation for analog transmission was investigated in [4]. In both cases, the optimal power allocation is similar to water-filling, i.e., sensor nodes with poor channel gains or noisy observations remain inactive to save power. The work of [4] was extended to the case of distributed estimation of a random field in [5]. A suboptimal power allocation scheme for the estimation of a random parameter in the presence of noisy links was proposed in [6].

In this paper, we investigate the problem of power allocation in a WSN using amplify-and-forward transmission to the fusion center (FC) as in [4]; however, rather than a scalar model, we consider a linear matrix-vector model used for field reconstruction based on shift-invariant spaces. Different from [4], this model makes the optimal power allocation depend on the sensor node positions. We formulate the optimal (in the mean square error sense) power allocation as a convex optimization problem that can be solved numerically using standard techniques. For the special case of critical sampling, we derive a closed-form solution.

Our paper is organized as follows. In Section II, we give a short introduction to shift-invariant spaces. Section III reviews our system architecture for field reconstruction in WSN. In Section IV, we study the optimal power allocation for field reconstruction in WSN. Section V shows some numerical results illustrating the performance of our power allocation scheme, and Section VI gives some concluding remarks.

The work was carried out within the framework of the FP7 Network of Excellence NEWCOM++ (Grant Agreement 216715), FWF Grant N10606, and WWTF Grant ICT08-044.

II. Shift-Invariant Spaces and B-Splines

We first review some basic facts about shift-invariant spaces which we used for field reconstruction in WSN in our previous work. We will only give a short overview here, restricting the discussion to the 2-D case. A more extensive discussion can be found in [2] and the references therein.

A shift-invariant space $V(g)$ is a linear subspace[1] of $L^2(\mathbb{R}^2)$ comprising all fields that can be represented as weighted superposition of spatial translates of a generator function $g(x,y) \in L^2(\mathbb{R}^2)$, i.e.,

$$V(g) = \left\{ f \in L^2(\mathbb{R}^2) \colon f(x,y) = \sum_{(k,l)\in\mathbb{Z}^2} c_{k,l}\, g(x-kD_x, y-lD_y) \right\},$$

where $c_{k,l} \in l_2(\mathbb{Z}^2)$. Without loss of generality, we will assume $D_x = D_y = 1$ in what follows, i.e., the generators are located on the integer grid. This can always be ensured via an appropriate normalization of the spatial coordinates x and y. To guarantee the stability of the representation above, we assume that the set of translates $\{g(x-k, y-l)\}_{(k,l)\in\mathbb{Z}^2}$ forms a Riesz basis for $V(g)$ (see [7], [8]).

We note that shift-invariant spaces are not bandlimited (BL) in general, but BL spaces are obtained as a special case with the separable sinc-type generator function

$$g_{\text{BL}}(x,y) \triangleq \frac{\sin(B_x \pi x)}{B_x \pi x} \frac{\sin(B_y \pi y)}{B_y \pi y} \tag{1}$$

where B_x and B_y denote the spatial bandwidths. Note that (1) decays very slowly. Hence, the corresponding space $V(g_{\text{BL}})$ is non-local, i.e., in the sampling/reconstruction problem the value of $f(x,y)$ depends on coefficients that are arbitrarily far away from (x,y). This is often inconvenient and motivates the use of generator functions with compact support. The support of $g(x,y)$ is defined as

$$\mathcal{S} = \operatorname{supp} g(x,y) \triangleq \operatorname{cl}\left\{(x,y) \in \mathbb{R}^2 : \ |g(x,y)| > 0\right\},$$

[1]We denote the space of square-integrable 2-D functions by $L^2(\mathbb{R}^2) = \{f(x,y) : \iint_{\mathbb{R}^2} |f(x,y)|^2 dx\, dy\} < \infty$, and the space of square-summable 2-D sequences by $l_2(\mathbb{Z}^2) = \{c_{k,l} : \sum_{(k,l)\in\mathbb{Z}^2} |c_{k,l}|^2 < \infty\}$.

where $\mathrm{cl}\{\cdot\}$ denotes topological closure. Hence the support is the closure of the set of points (x, y) where the function $g(x, y)$ is non-zero. A particularly useful class of compactly supported generator functions is given by basis-splines (B-splines), which have minimal support with respect to a given degree. Specifically, we will use 2-D spline functions in the following, constructed as $b_N(x, y) = \tilde{b}_N(x)\tilde{b}_N(y)$, with the one-dimensional (1-D) splines of order N defined via the N-fold convolution

$$\tilde{b}_N(x) \triangleq \Pi(x) \underbrace{* \Pi(x) \ldots * \Pi(x)}_{N \text{ times}}. \tag{2}$$

Here, the rectangular function $\Pi(x) = \tilde{b}_0(x)$ is defined as

$$\Pi(x) \triangleq \begin{cases} 1, & |x| \leq \frac{1}{2}, \\ 0, & \text{else.} \end{cases}$$

Alternatively, the B-splines can be calculated using the *Cox-de Boor* recursion formula [9]. The support of the 2-D splines is given by $\mathcal{S} = \operatorname{supp} b_N(x, y) = [-S_N/2, S_N/2] \times [-S_N/2, S_N/2]$ with $S_N = N + 1$. Due to this compact support, the shift-invariant spaces $V(b_N)$ are not BL.

III. System Architecture

A. Signal Model

We consider a WSN consisting of I sensor nodes deployed over a given region $\mathcal{A}$ to monitor a 2-D physical field $h(x, y)$. Here, x and y denote the spatial coordinates. The position of sensor node i is given by (x_i, y_i) and its measurement reads $h(x_i, y_i) + v_i$; here, v_i denotes spatially white measurement noise with variance $\sigma^2_{v_i}$. We assume that the physical field has mean power σ^2_h and moreover $h(x, y) \in V(b_N)$, i.e.,

$$h(x, y) = \sum_{(k,l)\in\mathbb{A}} c_{k,l}\, b_N(x-k, y-l),$$

where $\mathbb{A} = \mathbb{Z}^2 \cap (\mathcal{A} + \mathcal{S})$. Reconstructing $h(x, y)$ from the measurements thus amounts to determining the coefficients $c_{k,l}$.

We adopt an amplify-and-forward (AF) transmission strategy where each sensor node transmits the scaled measurement $\sqrt{p_i}\big(h(x_i, y_i)+v_i\big)$ to the FC. The average transmit power of sensor node i thus equals $P_i = p_i\big(\sigma^2_h + \sigma^2_{v_i}\big)$. The sum power $\sum_{i=1}^{I} P_i$ is constraint to be at most equal to P_{T}. The transmissions of the individual sensor nodes are over orthogonal channels and the signals received by the FC are given by

$$r_i = \sqrt{\gamma_i}\sqrt{p_i}\big(h(x_i, y_i) + v_i\big) + w_i = \sqrt{\gamma_i p_i}h(x_i, y_i) + z_i.$$

Here, γ_i is the channel gain, which will be used below to model Gaussian channels ($\gamma_i = 1$) and flat Rayleigh fading channels (exponentially distributed γ_i with mean μ_γ). Furthermore, w_i is white receiver noise with variance σ^2_w and

$$z_i = \sqrt{\gamma_i p_i} v_i + w_i \tag{3}$$

denotes the aggregate noise with variance $\gamma_i p_i \sigma^2_{v_i} + \sigma^2_w$.

We next formulate the system model using matrices and vectors. To this end, let (k_0, l_0) and (k_1, l_1) denote the smallest and largest indices in $\mathbb{A}$, respectively, such that $J = KL$ with $K \triangleq k_1 - k_0 + 1$ and $L \triangleq (l_1 - l_0 + 1)$. We define the block-banded $I \times J$ matrix $\mathbf{G}$ with elements

$$[\mathbf{G}]_{i,p} = b_N(x_i - k_p,\, y_i - l_p)$$

and the vectors $\mathbf{r}, \mathbf{v}$ (length I), and $\mathbf{c}$ (length J) with elements

$$[\mathbf{r}]_i = r_i, \;\; [\mathbf{v}]_i = v_i, \;\; \text{and} \;\; [\mathbf{c}]_p = c_{k_p, l_p},$$

where $k_p = k_0 + ((p\text{–}1) \bmod K)$, and $l_p = l_0 + \big\lfloor \frac{p-1}{K} \big\rfloor$. Accordingly, the receive signals can be rewritten in matrix-vector form as

$$\mathbf{r} = \mathbf{A}\mathbf{G}\mathbf{c} + \mathbf{z} = \tilde{\mathbf{G}}\mathbf{c} + \mathbf{z}, \tag{4}$$

where $\mathbf{A} \triangleq \mathrm{diag}\,\{\sqrt{\gamma_i p_i}\}$, $\tilde{\mathbf{G}} \triangleq \mathbf{A}\mathbf{G}$, and the aggregate noise vector $\mathbf{z}$ has covariance matrix $\mathbf{C}_{\mathbf{z}} = \mathrm{diag}\,\big\{\gamma_i p_i \sigma^2_{v_i} + \sigma^2_w\big\}$ (cf. (3)).

B. Field Reconstruction and Reconstruction Performance

We determine the field coefficients $\mathbf{c}$ in the linear system model (4) using the best linear unbiased estimator (BLUE) with the noise covariance matrix $\mathbf{C}_{\mathbf{z}}$ as weight, i.e.,

$$\hat{\mathbf{c}} \triangleq \arg\min_{\mathbf{c}} \|\tilde{\mathbf{G}}\mathbf{c} - \mathbf{r}\|^2_{\mathbf{C}^{-1}_{\mathbf{z}}} = (\tilde{\mathbf{G}}^T\mathbf{C}^{-1}_{\mathbf{z}}\tilde{\mathbf{G}})^{-1}\tilde{\mathbf{G}}^T\mathbf{C}^{-1}_{\mathbf{z}}\mathbf{r}. \tag{5}$$

Note that the computation of the coefficient estimates $\hat{\mathbf{c}}$ requires that the noise statistics $\mathbf{C}_{\mathbf{z}}$ and the matrix $\tilde{\mathbf{G}}$ (i.e., the sensor node positions and channel gains) are known at the FC.

In order for this solution to exist, the matrix $\tilde{\mathbf{G}}$ must have full rank, which in turn requires $I \geq J$, i.e., that there are at least as many sensor nodes as unknown coefficients and the sensor nodes are sufficiently closely spaced. Technically, the sensor node positions (x_i, y_i), have to form a so-called stable sampling set (see [8]). We note that the case $I = J$ is referred to as critical sampling.

With the optimal coefficient estimates (5), the field can be reconstructed for $(x, y) \in \mathcal{A}$ according to

$$\hat{h}(x, y) = \sum_{(k,l)\in\mathbb{A}} \hat{c}_{k,l}\, b_N(x-k, y-l). \tag{6}$$

To assess the the quality of the field reconstruction (6), we next derive the mean-square field reconstruction error within $\mathcal{A}$:

$$\begin{aligned}
\varepsilon &= \mathrm{E}\left\{ \iint_{\mathcal{A}} \Big(\hat{h}(x, y) - h(x, y)\Big)^2 \, dx\, dy \right\} \\
&= \mathrm{E}\left\{ \iint_{\mathcal{A}} \Big((\hat{\mathbf{c}} - \mathbf{c})^T\, \mathbf{g}(x, y)\Big)^2 \, dx\, dy \right\} \\
&= \iint_{\mathcal{A}} \mathbf{g}^T(x, y)\, \mathrm{E}\left\{ (\hat{\mathbf{c}} - \mathbf{c})\, (\hat{\mathbf{c}} - \mathbf{c})^T \right\} \mathbf{g}(x, y) dx\, dy \\
&= \iint_{\mathcal{A}} \mathrm{tr}\left\{ \mathbf{C}_{\hat{\mathbf{c}}-\mathbf{c}} \mathbf{g}(x, y)\mathbf{g}^T(x, y) \right\} dx\, dy \\
&= \mathrm{tr}\Big\{ \mathbf{C}_{\hat{\mathbf{c}}-\mathbf{c}} \iint_{\mathcal{A}} \mathbf{g}(x, y)\mathbf{g}^T(x, y)\, dx\, dy \Big\} \\
&= \mathrm{tr}\left\{ \mathbf{C}_{\hat{\mathbf{c}}-\mathbf{c}} \mathbf{G}_{\mathbf{g}} \right\}.
\end{aligned} \tag{7}$$

Here, the expectation was taken with respect to the noise and we used the length-J vector $\mathbf{g}(x, y)$ defined via its elements

$$[\mathbf{g}]_p(x, y) = g(x - k_p, y - l_p),$$

with k_p and l_p as in Section III-A; furthermore, $\mathbf{G}_{\mathbf{g}} = \iint_{\mathcal{A}} \mathbf{g}(x, y)\mathbf{g}^T(x, y)\, dx\, dy$ denotes the Gramian of $\mathbf{g}(x, y)$ and $\mathbf{C}_{\hat{\mathbf{c}}-\mathbf{c}} = \mathrm{E}\big\{(\hat{\mathbf{c}} - \mathbf{c})(\hat{\mathbf{c}} - \mathbf{c})^T\big\}$ is the correlation matrix of the coefficient error $\hat{\mathbf{c}} - \mathbf{c}$. When using B-splines as generator functions, the Gramian $\mathbf{G}_{\mathbf{g}}$ can be shown to be a symmetric block-banded Toeplitz matrix[2], where the band structure results from the compact

[2] A symmetric block-banded Toeplitz matrix is a symmetric Toeplitz matrix consisting of blocks that are banded and have Toeplitz structure as well.

support of the B-spline functions. The correlation matrix of the estimation error can be developed as

$$\begin{aligned}\mathbf{C}_{\hat{\mathbf{c}}-\mathbf{c}} &= \operatorname{cov}\left\{(\tilde{\mathbf{G}}^T\mathbf{C}_{\mathbf{z}}^{-1}\tilde{\mathbf{G}})^{-1}\tilde{\mathbf{G}}^T\mathbf{C}_{\mathbf{z}}^{-1}\mathbf{z}\right\}\\ &= (\tilde{\mathbf{G}}^T\mathbf{C}_{\mathbf{z}}^{-1}\tilde{\mathbf{G}})^{-1} = (\mathbf{G}^T\mathbf{A}^T\mathbf{C}_{\mathbf{z}}^{-1}\mathbf{A}\mathbf{G})^{-1}\\ &= (\mathbf{G}^T\mathbf{D}\mathbf{G})^{-1}. \end{aligned} \tag{8}$$

Here, we used the diagonal matrix

$$\mathbf{D} \triangleq \mathbf{A}^T\mathbf{C}_{\mathbf{z}}^{-1}\mathbf{A} = \operatorname{diag}\{d_i\}, \quad \text{with } d_i \triangleq \frac{1}{\sigma_{v_i}^2 + \frac{\sigma_w^2}{\gamma_i p_i}}. \tag{9}$$

Inserting (8) and (9) into (7), we finally obtain the MSE as

$$\varepsilon = \operatorname{tr}\left\{\mathbf{C}_{\hat{\mathbf{c}}-\mathbf{c}}\mathbf{G}_{\mathbf{g}}\right\} = \operatorname{tr}\left\{(\mathbf{G}^T\mathbf{D}\mathbf{G})^{-1}\mathbf{G}_{\mathbf{g}}\right\}. \tag{10}$$

This expressions captures the dependence of the reconstruction MSE on the channel gains γ_i, the sensor node positions (x_i, y_i), the AF factors p_i, and the noise variances $\sigma_{v_i}^2$ and σ_w^2.

C. Gaussian Channels and Identical Noise Variances

We next take a closer look at a special case for which it is easier to calculate the MSE and to assess its dependence on the individual parameters. We assume Gaussian channels, i.e., $\gamma_i = 1$ for all i, identical measurement noise variance $\sigma_{v_i}^2 = \sigma_v^2$ at all sensor nodes, and uniform power allocation to the sensor nodes, i.e., $p_i = \frac{P}{I}$ where $P = P_{\mathrm{T}}/(\sigma_h^2 + \sigma_v^2)$. It then follows that $\mathbf{D} = d\mathbf{I}$ with

$$d \triangleq \frac{1}{\sigma_v^2 + \frac{\sigma_w^2 I}{P}},$$

and therefore

$$\begin{aligned}\varepsilon &= \operatorname{tr}\left\{(\mathbf{G}^T d\mathbf{I}\mathbf{G})^{-1}\mathbf{G}_{\mathbf{g}}\right\} = \frac{1}{d}\operatorname{tr}\left\{(\mathbf{G}^T\mathbf{G})^{-1}\mathbf{G}_{\mathbf{g}}\right\}\\ &= \left(\sigma_v^2 + \frac{\sigma_w^2 I}{P}\right)\operatorname{tr}\left\{(\mathbf{G}^T\mathbf{G})^{-1}\mathbf{G}_{\mathbf{g}}\right\}.\end{aligned}$$

It can be seen that under the above assumptions the MSE is a product of two terms, one of which is completely determined by the measurement and receiver noise and by the per-sensor node transmit power; the other term depends only on the generator function and the sensor node placement (via $\mathbf{G}$). Note that in spite of identical channel gains and noise variances, the uniform power allocation is still suboptimal in this case because it does not take into account the influence of the sensor node positions on the reconstruction error.

IV. Optimal Power Allocation

A. General Case

We aim at allocating the power scaling factors p_i such that the reconstruction MSE in (10) is minimized subject to a sum power constraint. Defining the length-I vectors $\mathbf{p} = (p_1 \ \dots \ p_I)^T$ and $\mathbf{q} = (q_1 \ \dots \ q_I)^T$ with $q_i = \sigma_h^2 + \sigma_{v_i}^2$ allows us to write the sum transmit power as

$$\sum_{i=1}^{I} p_i(\sigma_h^2 + \sigma_{v_i}^2) = \mathbf{p}^T\mathbf{q}.$$

Recalling that P_{T} is the maximal sum power, we thus have

$$\begin{aligned}\underset{\mathbf{p}\in\mathbb{R}_+^I}{\text{minimize}} \quad & \operatorname{tr}\left\{(\mathbf{G}^T\mathbf{D}(\mathbf{p})\mathbf{G})^{-1}\mathbf{G}_{\mathbf{g}}\right\}\\ \text{subject to} \quad & \mathbf{p}^T\mathbf{q} \le P_{\mathrm{T}},\end{aligned} \tag{11}$$

where we made the dependence of $\mathbf{D}$ on $\mathbf{p}$ explicit by writing $\mathbf{D}(\mathbf{p})$. The power allocated to sensor node i depends on the local measurement noise variance $\sigma_{v_i}^2$, the channel gain γ_i, and (through the matrix $\mathbf{G}$) the sensor node positions.

The optimization problem (11) is a variation of the well-known A-optimal convex problem (see the Appendix for more details). While in general this problem has no closed-form solution, it can be solved numerically in an efficient manner.

B. Critical Sampling

In some applications the numerical solution of the power allocation problem may still be too expensive for a low-complexity and low-energy FC. Thus, we next study in more detail the special case of critical sampling ($I = J$), for which we show that the power allocation problem has a closed-form solution. We assume that the $I = J$ sensor nodes form a stable sampling set such that $\mathbf{G}$ is a square invertible matrix. This allows us to simplify (10) as

$$\begin{aligned}\varepsilon &= \operatorname{tr}\left\{(\mathbf{G}^T\mathbf{D}\mathbf{G})^{-1}\mathbf{G}_{\mathbf{g}}\right\} = \operatorname{tr}\left\{\mathbf{G}^{-1}\mathbf{D}^{-1}(\mathbf{G}^T)^{-1}\mathbf{G}_{\mathbf{g}}\right\}\\ &= \operatorname{tr}\left\{\mathbf{D}^{-1}(\mathbf{G}^T)^{-1}\mathbf{G}_{\mathbf{g}}\mathbf{G}^{-1}\right\} = \sum_{i=1}^{I}\frac{1}{d_i}g_i\\ &= \sum_{i=1}^{I}\sigma_{v_i}^2 g_i + \sum_{i=1}^{I}\frac{\sigma_w^2 g_i}{\gamma_i p_i},\end{aligned} \tag{12}$$

where we defined $g_i \triangleq \left[(\mathbf{G}^T)^{-1}\mathbf{G}_{\mathbf{g}}\mathbf{G}^{-1}\right]_{ii}$ and used that $\mathbf{D}^{-1} = \operatorname{diag}\{d_i^{-1}\}$ with $d_i^{-1} = \left(\sigma_{v_i}^2 + \frac{\sigma_w^2}{\gamma_i p_i}\right)$ (cf. (9)).

Since the first sum in (12) is independent of the power scaling factors p_i, the optimization problem in (11) simplifies to

$$\begin{aligned}\underset{\mathbf{p}\in\mathbb{R}_+^J}{\text{minimize}} \quad & \sum_{i=1}^{J}\frac{\sigma_w^2 g_i}{\gamma_i p_i}\\ \text{subject to} \quad & \mathbf{p}^T\mathbf{q} \le P_{\mathrm{T}}.\end{aligned} \tag{13}$$

The Lagrangian associated to this problem equals

$$\begin{aligned}L(\mathbf{p},\lambda) &= \sum_{i=1}^{I}\frac{\sigma_w^2 g_i}{\gamma_i p_i} + \lambda\left(\mathbf{p}^T\mathbf{q} - P_{\mathrm{T}}\right)\\ &= \sum_{i=1}^{I}\left(\frac{\sigma_w^2 g_i}{\gamma_i p_i} + \lambda p_i q_i\right) - \lambda P_{\mathrm{T}}\end{aligned}$$

and the Lagrangian dual function denotes

$$\begin{aligned}g(\lambda) &= L(\mathbf{p}^\star,\lambda) = \inf_{\mathbf{p}} L(\mathbf{p},\lambda)\\ &= \sum_{i=1}^{I}\inf_{p_i}\left(\frac{\sigma_w^2 g_i}{\gamma_i p_i} + \lambda p_i q_i\right) - \lambda P_{\mathrm{T}}\\ &= \sum_{i=1}^{I}\left(\frac{\sigma_w^2 g_i}{\gamma_i p_i^\star} + \lambda p_i^\star q_i\right) - \lambda P_{\mathrm{T}}\\ &= 2\sigma_w\sqrt{\lambda}\sum_{i=1}^{I}\sqrt{\frac{g_i q_i}{\gamma_i}} - \lambda P_{\mathrm{T}},\end{aligned}$$

where

$$p_i^\star = \arg\inf_{p_i}\left(\frac{\sigma_w^2 g_i}{\gamma_i p_i} + \lambda p_i q_i\right) = \sqrt{\frac{\sigma_w^2 g_i}{\lambda\gamma_i q_i}}.$$

We therefore have the Lagrange dual problem

$$\begin{aligned}\underset{\lambda}{\text{maximize}} \quad & 2\sigma_w\sqrt{\lambda}\sum_{i=1}^{I}\sqrt{\frac{g_i q_i}{\gamma_i}} - \lambda P_{\mathrm{T}}\\ \text{subject to} \quad & \lambda \ge 0,\end{aligned}$$

whose solution is given by

$$\lambda^\star = \frac{\sigma_w^2\left(\sum_{i=1}^{I}\sqrt{\frac{g_i q_i}{\gamma_i}}\right)^2}{P_{\mathrm{T}}^2}.$$

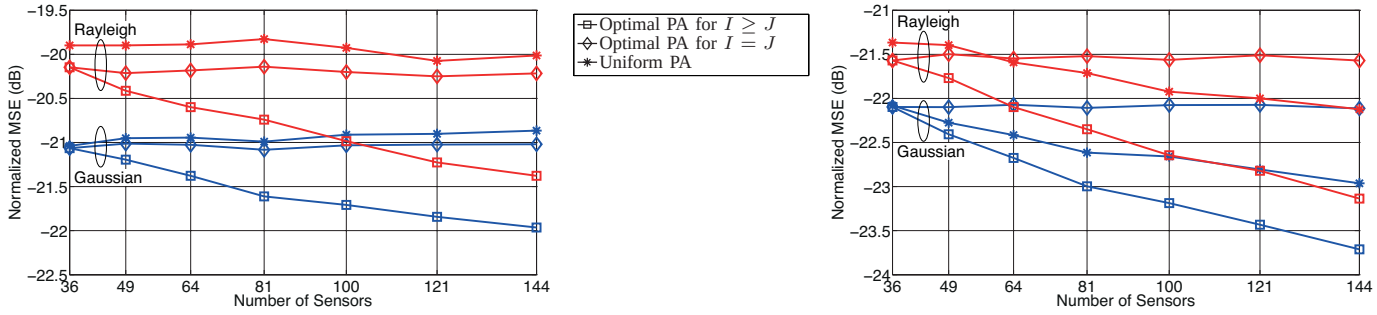

(a) (b)

Fig. 1. Comparison of the reconstruction performance for various power allocations in terms of normalized MSE versus numbers of sensor nodes I in Gaussian and Rayleigh fading channels: (a) low sum power ($P_{\mathrm{T}} = 10$), (b) high sum power ($P_{\mathrm{T}} = 100$).

It can be shown that the KKT conditions [10] hold for our convex problem, which is a sufficient condition for strong duality. With the dual optimal solution $\lambda^\star$, the optimal solution for the primal problem equals $L(\mathbf{p}^\star, \lambda^\star) = g(\lambda^\star)$ with the (primal feasible) minimizer

$$p_i^\star = P_{\mathrm{T}} \frac{\sqrt{\frac{g_i}{\gamma_i q_i}}}{\sum_{j=1}^{I} \sqrt{\frac{g_j q_j}{\gamma_j}}} = P_{\mathrm{T}} \frac{\sqrt{\frac{g_i}{\gamma_i(\sigma_h^2+\sigma_{v_i}^2)}}}{\sum_{j=1}^{I} \sqrt{\frac{g_j(\sigma_h^2+\sigma_{v_j}^2)}{\gamma_j}}}. \tag{14}$$

It can be seen from (14) that every sensor node is allocated non-zero power; this ensures $I \geq J$ and hence that the stable sampling set is preserved. With the definition $\beta_i \triangleq \sqrt{\frac{g_i(\sigma_h^2+\sigma_{v_i}^2)}{\gamma_i}}$, the optimal transmit powers can be written as

$$P_i^\star = p_i^\star(\sigma_h^2 + \sigma_{v_i}^2) = \alpha_i P_{\mathrm{T}}, \quad \text{with } \alpha_i \triangleq \frac{\beta_i}{\sum_{j=1}^{I} \beta_j}.$$

Here, α_i is the fraction of power used by sensor node i; this fraction is large if g_i is large (which means that sensor node i is rather isolated) or if the associated channel gain γ_i is small. Hence, the optimal power allocation compensates for poor channel or sampling conditions. It is worth noting that the power fraction α_i becomes large also when the associated measurement noise variance $\sigma_{v_i}^2$ is large; as can be verified from (14), the optimal power scaling $p_i^\star$ in this case is small, i.e., the large transmit power is solely due to the fact that the power of the measurement is already large.

It is interesting to reconsider the case of Gaussian channels and identical measurement noise variance from Section III-C. Here, $\alpha_i \triangleq \frac{\sqrt{g_i}}{\sum_{j=1}^{I} \sqrt{g_j}}$ and the power allocation is not uniform unless all g_i are identical, i.e., unless the sensor nodes are placed on a regular lattice.

V. Numerical Simulations

We next present numerical results to illustrate the performance of our power allocation strategies. We consider a shift-invariant space using a B-spline of order $N = 3$ and normalized the field such that the average power equals $\sigma_h^2 = 1$. The region being sensed is $\mathcal{A} = [0, 5] \times [0, 5]$ (i.e., $J = 36$ field coefficients). We used a WSN deployment with $I \geq 36$ sensor nodes, where the first $J = 36$ sensor nodes (the minimum number) are placed on a rectangular grid and the remaining $I - J$ sensor nodes are randomly placed according to a spatially uniform distribution over the region $\mathcal{A}$. Since the first J sensor nodes form a stable sampling set, the entire WSN of I sensor nodes does so too. The measurement noise variance at the different sensor nodes was chosen according to a uniform distribution, i.e., $\sigma_{v_i}^2 \sim \mathrm{Unif}\{0.01, 0.1\}$ (this corresponds to measurement SNRs between 10 dB and 20 dB). For the Gaussian channel case we set the channel gains $\gamma_i = 1$, whereas for the Rayleigh-fading channel we generated exponentially distributed γ_i with mean $\mu_\gamma = 1$. For each scenario, we chose the receiver noise variance as $\sigma_w^2 \sim \mathrm{Unif}\{0.01, 0.1\}$. We further consider two setups with low sum power ($P_{\mathrm{T}} = 10$) and with high sum power ($P_{\mathrm{T}} = 100$).

Using the parameters specified above, our simulations compare three power allocation schemes: (i) the numerically evaluated optimal power allocation scheme according to (11); (ii) power allocation according to the closed-form expression (14) for the first 36 sensor nodes and zero power for the remaining sensor nodes; (iii) a baseline scheme with uniform power allocation, i.e., $P_i = P_{\mathrm{T}}/I$.

Fig. 1 displays the normalized field reconstruction MSE versus the number of sensor nodes I for both sum power levels. It is seen that the optimal power allocation performs best for all numbers of sensor nodes and that its performance advantage over the other two schemes increases with increasing I. The performance of the power allocation (14) is independent of I since only the first $J = 36$ sensor nodes have non-zero power, i.e., the remaining sensors remain silent. This power allocation is superior to uniform power allocation at low sum power but tends to be inferior to uniform allocation at high sum power (specifically for large I).

Fig. 2 depicts an example of how the sensor node powers P_i are allocated in the case of a Gaussian channel and $I = 64$. We divide the sensor nodes into two groups (sensor nodes 1–36 and 37–64) and sort the sensor nodes within each group according to increasing noise variance $\sigma_{v_i}^2$. That way, the impact of the sensor node positions is easier to identify. The power allocation for the critically sampled case (using only sensor nodes 1–36) and low sum power is shown in Fig. 2(a). Clearly, higher measurement noise power tends to scale up the transmit power (even if the power scaling factor p_i is smaller); however, the power increase is not monotonic due to the additional impact of the sensor node position. For low sum-power, the optimal power allocation is shown Fig. 2(b). The largest part of power is again allocated to sensor nodes 1–36 due to their good localization on a regular grid; in this power-limited regime, only few sensor nodes in the second group (those with favorable position and measurement noise) have non-negligible power. For the high power scenario shown in Fig. 2(c), power is allocated more evenly to all sensor nodes even though a large fraction of the sum power is still allocated to the first group of sensor nodes.

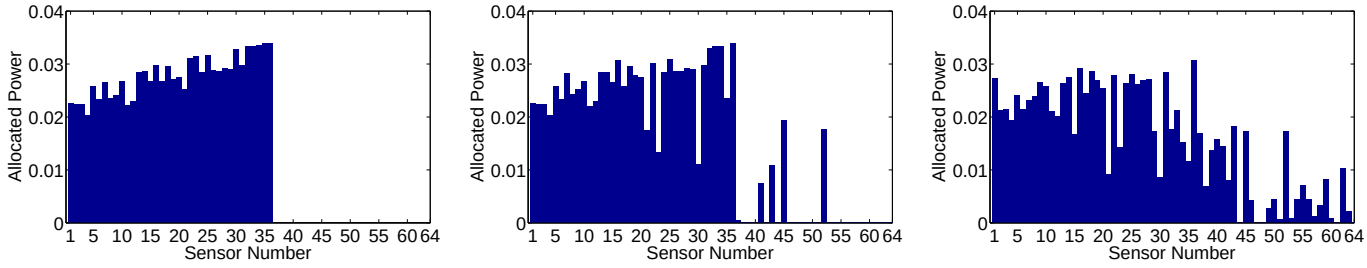

(a) (b) (c)

Fig. 2. Example for the power allocation in a WSN with $I = 64$ sensor nodes and Gaussian channels. The plots displays the fraction of power α_i versus sensor node number for (a) optimal power allocation for the first group of 36 sensor nodes and low sum power ($P_{\mathrm{T}} = 10$); (b) optimal allocation for low sum power ($P_{\mathrm{T}} = 10$), and (c) optimal allocation for high sum power ($P_{\mathrm{T}} = 100$). The sensor nodes within each group (sensor nodes 1–36 and 37–64) are sorted according to increasing noise variance $\sigma_{v_i}^2$.

VI. Conclusions

We considered field reconstruction in WSN based on shift-invariant spaces and an amplify-and-forward protocol for the transmission of sensor node measurements to the fusion center. We derived the MSE achieved by this scheme and developed an MSE-optimal power allocation scheme. For the case of critical sampling, the optimal power allocation was expressed in closed form. Numerical simulations for Gaussian and Rayleigh fading channels demonstrated how power is allocated to the sensor nodes and how this impacts the overall field reconstruction quality.

Using the optimal power allocation scheme for the critically sampled case by using only $J \leq I$ sensor nodes is clearly suboptimal since many sensor measurements remain unused. This drawback can be circumvented by splitting the WSN into sub-WSN of size J, i.e., considering stable sampling subsets of the I sensor nodes and applying the power allocation for critically sampling to each sub-WSN. One option then is to impose a round-robin (serial) scheduling where the sub-WSN are alternately used for reconstruction. This reduces the energy consumption because inactive sensor nodes can temporarily be switched off while it is assured that over time all sensor nodes are used in the reconstruction process. The second option is to use a parallel scheduling, i.e., the sub-WSN simultaneously contribute to the reconstruction by allocating the power to the sensor nodes of the sub-WSN according to (14) and by averaging the results obtained by the different sub-WSN (see [11]). That way, all sensor nodes are active all the time, achieving a better reconstruction quality at the expense of larger energy consumption. Serial and parallel schedules could as well be combined to achieve a trade-off between energy consumption and reconstruction quality.

Appendix A
Optimization Problem Revisited

The matrix $\mathbf{G_g}$ is positive definite and can hence be factorized as $\mathbf{G_g} = \mathbf{G_g}^{1/2}\mathbf{G_g}^{1/2}$, where $\mathbf{G_g}^{1/2}$ is again positive definite and hence invertible [12]. The MSE of the reconstructed field in (10) can thus be rewritten as

$$\begin{aligned}\varepsilon &= \mathrm{tr}\left\{(\mathbf{G}^T\mathbf{D}\mathbf{G})^{-1}\mathbf{G_g}\right\}\\ &= \mathrm{tr}\left\{(\mathbf{G}^T\mathbf{D}\mathbf{G})^{-1}\mathbf{G_g}^{1/2}\mathbf{G_g}^{1/2}\right\}\\ &= \mathrm{tr}\left\{\mathbf{G_g}^{1/2}(\mathbf{G}^T\mathbf{D}\mathbf{G})^{-1}\mathbf{G_g}^{1/2}\right\}\\ &= \mathrm{tr}\left\{\left(\mathbf{G_g}^{-1/2}\mathbf{G}^T\mathbf{D}\mathbf{G}\mathbf{G_g}^{-1/2}\right)^{-1}\right\}\\ &= \mathrm{tr}\left\{\left(\sum_{i=1}^{I} d_i\mathbf{G_g}^{-1/2}\mathbf{g}_i\mathbf{g}_i^T\mathbf{G_g}^{-1/2}\right)^{-1}\right\}\\ &= \mathrm{tr}\left\{\left(\sum_{i=1}^{I} d_i\mathbf{u}_i\mathbf{u}_i^T\right)^{-1}\right\},\end{aligned}$$

where $\mathbf{g}_i$ denotes the columns of $\mathbf{G}^T$ and $\mathbf{u}_i = \mathbf{G_g}^{-1/2}\mathbf{g}_i$. Further using the one-to-one correspondence $p_i = \frac{\sigma_w^2 d_i}{\gamma_i(1-\sigma_{v_i}^2 d_i)}$ and introducing the slack variable $\mathbf{s} = (s_1 \ \ldots \ s_J)^T$, the problem in (11) can be cast as [10]

$$\begin{aligned}\underset{\mathbf{s},\mathbf{d}}{\text{minimize}} \quad & \mathbf{1^T s}\\ \text{subject to} \quad & \begin{bmatrix}\sum_i^I d_i\mathbf{u}_i\mathbf{u}_i^T & \mathbf{e}_p\\ \mathbf{e}_p^T & s_p\end{bmatrix} \succeq 0\\ & \mathbf{d} \succeq 0\\ & \sigma_w^2\sum_{i=1}^{I}\frac{d_i(\sigma_h^2+\sigma_{v_i}^2)}{\gamma_i(1-\sigma_{v_i}^2 d_i)} \leq P_{\mathrm{T}}\\ & d_i - \frac{1}{\sigma_{v_i}^2} \leq 0.\end{aligned} \tag{15}$$

Here $\mathbf{e}_p$ is the pth unit vector and the last inequality ensures $p_i \geq 0$.

References

[1] M. Gastpar, M. Vetterli, and P. L. Dragotti, "Sensing reality and communicating bits: a dangerous liaison," *IEEE Signal Process. Mag.*, vol. 23, no. 4, pp. 70–83, Jul. 2006.

[2] G. Reise and G. Matz, "Distributed sampling and reconstruction of non-bandlimited fields in sensor networks based on shift invariant spaces," in *Proc. ICASSP 2009*, Taipeh, Taiwan, Apr. 2009, pp. 2061–2064.

[3] J.-J. Xiao, S. Cui, Z.-Q. Luo, and A. Goldsmith, "Power scheduling of universal decentralized estimation in sensor networks," *IEEE Trans. Signal Process.*, vol. 54, no. 2, pp. 413–422, Feb. 2006.

[4] S. Cui, J.-J. Xiao, A. Goldsmith, Z.-Q. Luo, and H. V. Poor, "Estimation diversity and energy efficiency in distributed sensing," *IEEE Trans. Signal Process.*, vol. 55, no. 9, pp. 4683–4695, Sep. 2007.

[5] I. Bahceci and A. Khandani, "Linear estimation of correlated data in wireless sensor networks with optimum power allocation and analog modulation," *IEEE Trans. Commun.*, vol. 56, no. 7, pp. 1146–1156, Jul. 2008.

[6] J. Fang and H. Li, "Power constrained distributed estimation with correlated sensor data," *IEEE Trans. Signal Process.*, vol. 57, no. 8, pp. 3292–3297, August 2009.

[7] O. Christensen, *An introduction to Frames and Riesz bases*. Birkhäuser, 2003.

[8] K. Gröchenig and H. Schwab, "Fast local reconstruction methods for nonuniform sampling in shift-invariant spaces," *SIAM J. Matrix Anal. Appl.*, vol. 24, no. 4, pp. 899–913, April 2003.

[9] C. de Boor, *A Practical Guide to Splines*, 2nd ed. Springer Verlag, 2001.

[10] S. Boyd and L. Vandenberghe, *Convex Optimization*. Cambridge University Press, 2004.

[11] G. Reise, G. Matz, and K. Gröchenig, "Distributed field reconstruction in wireless sensor networks based on hybrid shift-invariant spaces," *to be submitted to IEEE Trans. Signal Process.*, 2011.

[12] R. A. Horn and C. R. Johnson, *Matrix Analysis*. Cambridge University Press, 1990.